AMERICAN SOCIETY FOR MICROBIOLOGY | Applied and Environmental Microbiology

Involvement of the Type IX Secretion System in *Capnocytophaga ochracea* Gliding Motility and Biofilm Formation

Daichi Kita,[a] Satoshi Shibata,[b] Yuichiro Kikuchi,[c,d] Eitoyo Kokubu,[c,d] Koji Nakayama,[b] Atsushi Saito,[a,d] Kazuyuki Ishihara[c,d]

Department of Periodontology, Tokyo Dental College, Tokyo, Japan[a]; Division of Microbiology and Oral Infection, Department of Molecular Microbiology and Immunology, Nagasaki University Graduate School of Biomedical Sciences, Nagasaki, Japan[b]; Department of Microbiology, Tokyo Dental College, Tokyo, Japan[c]; Oral Health Science Center, Tokyo Dental College, Tokyo, Japan[d]

Capnocytophaga ochracea* is a Gram-negative, rod-shaped bacterium that demonstrates gliding motility when cultured on solid agar surfaces. *C. ochracea* possesses the ability to form biofilms; however, factors involved in biofilm formation by this bacterium are unclear. A type IX secretion system (T9SS) in *Flavobacterium johnsoniae* was shown to be involved in the transport of proteins (e.g., several adhesins) to the cell surface. Genes orthologous to those encoding T9SS proteins in *F. johnsoniae* have been identified in the genome of *C. ochracea*; therefore, the T9SS may be involved in biofilm formation by *C. ochracea*. Here we constructed three ortholog-deficient *C. ochracea* mutants lacking *sprB* (which encodes a gliding motility adhesin) or *gldK* or *sprT* (which encode T9SS proteins in *F. johnsoniae*). Gliding motility was lost in each mutant, suggesting that, in *C. ochracea*, the proteins encoded by *sprB*, *gldK*, and *sprT* are necessary for gliding motility, and SprB is transported to the cell surface by the T9SS. For the Δ*gldK*, Δ*sprT*, and Δ*sprB* strains, the amounts of crystal violet-associated biofilm, relative to wild-type values, were 49%, 34%, and 65%, respectively, at 48 h. Confocal laser scanning and scanning electron microscopy revealed that the biofilms formed by wild-type *C. ochracea* were denser and bacterial cells were closer together than in those formed by the mutant strains. Together, these results indicate that proteins exported by the T9SS are key elements of the gliding motility and biofilm formation of *C. ochracea*.

Capnocytophaga ochracea is a Gram-negative, rod-shaped bacterium that demonstrates gliding motility when cultured on solid agar surfaces (1–3). *C. ochracea* was first isolated from human periodontitis lesions (4–6); however, subsequent studies have indicated that this bacterium is present in dental plaque from periodontally healthy sites (7). Although a recent metatranscriptome analysis has shown that putative virulence factors of *C. ochracea* are upregulated in patients with periodontitis (8), the role of *C. ochracea* in the pathogenesis and progression of periodontal disease remains controversial (9–13). *C. ochracea* is also reported to be involved in several systemic diseases and to produce an immunosuppressive factor (14, 15). *C. ochracea* has been implicated in focal infections, such as sepsis and purpura fulminans (16, 17), and associations between high levels of antibodies to *C. ochracea* and coronary heart disease (18) and a potential relationship with Sjögren's syndrome (19) have been reported.

To clarify the involvement of *C. ochracea* in these diseases, investigation of the colonization strategies used by this bacterium is essential. *C. ochracea* colonizes tooth surfaces by forming a biofilm and synergizing its growth with that of *Fusobacterium nucleatum*, which acts as a bridge between antecedent bacteria on the tooth surface and late-colonizing periodontopathic bacteria (20). However, the factors involved in biofilm formation by this bacterium remain unknown. For *Escherichia coli*, it is thought that motility facilitates biofilm expansion by enabling growing cells to migrate across the surface on which they are growing (21). For *Pseudomonas aeruginosa*, flagella and pili are known to play important roles in the aggregation of bacterial cells and the formation of microcolonies (22). Thus, we hypothesized that the gliding motility of *C. ochracea* is an important aspect of its biofilm formation.

Recently, a novel protein secretion system, the type IX secretion system (T9SS), was identified in *Porphyromonas gingivalis* and other members of the phylum *Bacteroidetes*. For example, in *P. gingivalis*, which is a prominent periodontal pathogen, several T9SS proteins (e.g., PorK, PorL, and PorT) were found to be crucial for the secretion of major proteases (23–26). T9SS proteins have also been found in *Flavobacterium johnsoniae* (phylum *Bacteroidetes*) (23, 25, 27, 28), and orthologous genes encoding T9SS proteins have been found in the genome of *C. ochracea* (28).

In *F. johnsoniae*, SprB (colony-spreading protein B) allows the bacterium to attach to agar and glass surfaces and to move via gliding motility (29). *F. johnsoniae* mutants deficient in genes encoding T9SS proteins (e.g., *gldK*, *gldL*, and *sprT*) are unable to attach to and to glide across glass surfaces, presumably as a result of their inability to secrete SprB and other adhesins at their cell surfaces (30). Since *C. ochracea* harbors orthologous genes predicted to encode T9SS proteins such as GldK and SprT (28), it is possible that proteins exported by the T9SS are involved in the gliding motility and biofilm formation of *C. ochracea*.

Here we constructed *C. ochracea* mutants deficient in the genes orthologous to *gldK*, *sprT*, or *sprB* in *F. johnsoniae*, and we investigated the role of the T9SS in gliding motility and biofilm forma-

Received 22 October 2015 **Accepted** 30 December 2015

Accepted manuscript posted online 4 January 2016

Citation Kita D, Shibata S, Kikuchi Y, Kokubu E, Nakayama K, Saito A, Ishihara K. 2016. Involvement of the type IX secretion system in *Capnocytophaga ochracea* gliding motility and biofilm formation. Appl Environ Microbiol 82:1756–1766. doi:10.1128/AEM.03452-15.

Editor: J. L. Schottel, University of Minnesota

Address correspondence to Kazuyuki Ishihara, ishihara@tdc.ac.jp.

TABLE 1 Bacterial strains and plasmids used in the present study

Strain or plasmid	Description[a]	Reference or source
Bacterial strains		
Escherichia coli DH5α	Strain used for gene cloning	TaKaRa Bio Inc.
Capnocytophaga ochracea strains		
ATCC 27872	Wild type	ATCC
Δ*gldK* mutant	*ermF-ermAM* insertion mutation in Coch_0809 of ATCC 27872; Em^r	This study
Δ*sprT* mutant	*ermF-ermAM* insertion mutation in Coch_1748 of ATCC 27872; Em^r	This study
Δ*sprB* mutant	*ermF-ermAM* insertion mutation in Coch_0203 of ATCC 27872; Em^r	This study
Plasmids		
pVA2198	*ermF-ermAM*	27
pCR2.1-TOPO	3.9-kb vector for cloning PCR products; Km^r Amp^r	Invitrogen

[a] Antibiotic resistance phenotypes: Em^r, erythromycin resistant; Km^r, kanamycin resistant; Amp^r, ampicillin resistant.

tion. Our results indicated that proteins exported by the T9SS in *C. ochracea* are involved in gliding motility and biofilm formation.

MATERIALS AND METHODS

Bacterial strains, plasmids, and growth conditions. The bacterial strains and plasmids used in the present study are listed in Table 1. *C. ochracea* ATCC 27872 (wild-type strain) was cultured and maintained, using standard methods, at 37°C on blood agar plates containing tryptic soy agar (Becton Dickinson, Sparks, MD) supplemented with hemin (5 μg/ml), menadione (0.5 μg/ml), and 10% horse blood (Nippon Bio-Test Laboratories, Tokyo, Japan), under anaerobic conditions (80% N_2, 10% H_2, and 10% CO_2) in an anaerobic chamber (ANX-3; Hirasawa, Tokyo, Japan). *C. ochracea* mutants were cultured and maintained on blood agar plates containing 10 μg/ml erythromycin (Sigma-Aldrich, St. Louis, MO). *C. ochracea* strains were also grown at 37°C in tryptic soy broth (Becton Dickinson) supplemented with hemin (5 μg/ml) and menadione (0.5 μg/ml), under anaerobic conditions. *E. coli* DH5α was grown at 37°C in Luria-Bertani agar (Wako Pure Chemical Industries, Osaka, Japan), under aerobic conditions, and the plasmid-transformed strains of *E. coli* were grown in Luria-Bertani agar containing 25 μg/ml kanamycin (Sigma-Aldrich).

Construction of Δ*gldK*, Δ*sprT*, and Δ*sprB* mutant strains. The genomic nucleotide sequence of *C. ochracea* ATCC 27872 was obtained from the GenBank database (accession no. NC_013162). The *C. ochracea* sequences of *gldK* and *sprT* (Coch_0809 and Coch_1748, respectively) were obtained from the National Center for Biotechnology Information database (www.ncbi.nlm.nih.gov). The *C. ochracea* ortholog of the *F. johnsoniae* gene encoding the gliding motility protein SprB (31) was searched against the whole-genome sequence of *C. ochracea* in the National Center for Biotechnology Information database by means of a BLAST search. The *C. ochracea* DNA sequence obtained from the search was designated *sprB* (Coch_0203).

The primers used in the present study are listed in Table 2. To construct the Δ*sprT* mutant, the upstream and downstream sequences of the target gene were amplified by means of PCR from chromosomal DNA of *C. ochracea* ATCC 27872 with the primer pairs SprT-F1/SprT-R1 and SprT-F2/SprT-R2, respectively. The *ermF-ermAM* cassette was amplified from the pVA2198 plasmid (32) by using the primers EMD2 and EMU2. The *ermF-ermAM* cassette was inserted into the upstream and downstream fragments of the target genes by using an overlap extension PCR method (33).

Similarly, for the Δ*sprB* mutant, the upstream and downstream sequences of *sprB* were amplified by means of PCR from the chromosomal DNA with the primer pairs SprB-F1/SprB-R1 and SprB-F2/SprB-R2, respectively. For the Δ*gldK* mutant, the upstream and downstream sequences of the target gene were amplified by means of PCR from the chromosomal DNA with the primer pairs GldK-F1/GldK-R1 and GldK-F2/GldK-R2, respectively. The *ermF-ermAM* cassette was amplified from the pVA2198 plasmid with the primers EMSprB-F and EMSprB-R (for *sprB*) or EMD2 and EMU2 (for *gldK*) and then inserted into the upstream and downstream fragments as described for the Δ*sprT* mutant.

The PCR-fused fragments from *sprT* and *sprB* were cloned into

TABLE 2 Primers used in the present study

Primer	Sequence[a]
SprT-F1	5′-ACAGGATTAGATATCTCAGAAGGAA-3′
SprT-R1	5′-TGTTGCAAATACCGATGAGCTGCCCATACAAATTCAATGCTCCT-3′
SprT-F2	5′-CGTTACTAAAGGGAATGTAGCCCAATAGCCCTTGGACAAGTAACCTT-3′
SprT-R2	5′-CATTAGAAATGTTCTCGAATGAGAACTC-3′
EMD2	5′-GCTCATCGGTATTTGCAACATCATAG-3′
EMU2	5′-CTACATTCCCTTTAGTAACGTGTAACTTTC-3′
SprB-F1	5′-TTATAACGTAACGACTGACCCATTT-3′
SprB-R1	5′-AAGGGAATGTAGAATTATAGAGCTCAACGTGCCTATG-3′
SprB-F2	5′-ATACCGATGAGCAAAAGGAATATAATTCTGCCCAAAG-3′
SprB-R2	5′-ATCTACCACGAACAAGCGTATAGAG-3′
EMSprB-F	5′-AGCTCTATAATTCTACATTCCCTTTAGTAACGTGTAACTTTC-3′
EMSprB-R	5′-TATATTCCTTTTGCTCATCGGTATTTGCAACATCATAG-3′
GldK-F1	5′-GATGCCTACATTCAGTGTTGCCAAT-3′
GldK-R1	5′-TGTTGCAAATACCGATGAGCAGCTAGTACTAATAGTACAAGTAGCATTAC-3′
GldK-F2	5′-CGTTACTAAAGGGAATGTAGGCTCCTTACGGTATGACGCTTATTCCGAG-3′
GldK-R2	5′-TCATAGTAGACATATATTCATATGAATTCG-3′

[a] Underlined letters indicate overlap regions. All primers are from this study.

pCR2.1-TOPO (Invitrogen, Carlsbad, CA), and the plasmids were transformed into *E. coli* DH5α. Transformants were selected on Luria-Bertani agar plates containing kanamycin (25 μg/ml). Recombinant plasmid DNA was isolated and digested with EcoRI. The fragments obtained (*sprT* or *sprB*) and the PCR-fused fragments of *gldK* were introduced into *C. ochracea* ATCC 27872 by means of electroporation, as described below. Mid-logarithmic-phase *C. ochracea* ATCC 27872 cells were harvested from 100 ml of culture medium, washed three times with ice-cold distilled water, and suspended in 0.2 ml of 10% glycerol. Then, 10 μg of the DNA fragments was mixed with 40 μl of the cells, and the mixture was incubated on ice for 1 min before being transferred to a 0.1-cm electroporation cuvette (Bio-Rad Laboratories, Hercules, CA). Electroporation was performed with a Gene Pulser II (Bio-Rad) at settings of 1.8 kV, 25 μF, and 250 Ω. Immediately after electroporation, the cells were suspended in 1 ml of tryptic soy broth and incubated overnight at 37°C under anaerobic conditions. The cells were then plated on blood agar plates containing 10 μg/ml erythromycin and were incubated for 5 to 7 days at 37°C under anaerobic conditions. Correct gene replacement in erythromycin-resistant mutants was confirmed by means of PCR (data not shown).

Growth properties of the mutant strains in liquid culture. *C. ochracea* strains were grown for 2 days at 37°C on blood agar plates and were inoculated into tryptic soy broth. After reaching the early stationary phase, the culture was diluted with fresh medium to an optical density at 660 nm (OD_{660}) of 0.1. Samples of the diluted cultures (10 ml) were then incubated at 37°C under anaerobic conditions. Bacterial growth was monitored by measuring OD_{660} with a spectrophotometer (Mini Photo 518R; Taitec, Tokyo, Japan) at predetermined time points.

Microscopic observation of bacterial movement on solid agar and glass surfaces. The movement of bacterial cells on solid agar surfaces (i.e., colony spreading) was examined by using phase-contrast microscopy as described previously, with minor modifications (34). In brief, cells in the early stationary phase were suspended in fresh medium to an OD_{660} of 1.0. Five-microliter samples of the cell suspensions were then spotted on glass slides covered with a thin layer of tryptic soy agar (agar content, 3%) supplemented with hemin (5 μg/ml), menadione (0.5 μg/ml), and 0.1% yeast extract (Becton Dickinson). After incubation for 5 days at 37°C under anaerobic conditions, colony spreading was observed by using a stereomicroscope (SMZ800; Nikon, Tokyo, Japan) equipped with a digital camera.

The movement of *C. ochracea* over a glass surface was also examined by means of phase-contrast microscopy. *C. ochracea* strains were grown for 2 days at 37°C, under anaerobic conditions, in tryptic soy broth supplemented with 0.1% yeast extract (TSBYE), were dripped on tryptic soy agar supplemented with 0.1% yeast extract, and were incubated for 2 days at 37°C under anaerobic conditions. After incubation, the edges of the colonies were scraped off and resuspended in TSBYE. Tunnel slides were prepared as described previously, by using 5-mm-thick double-sided tape (NW-5; Nichiban, Tokyo, Japan) to hold a glass coverslip above a glass slide (35). Cells suspended in TSBYE were introduced into the tunnel slides, and fresh TSBYE was used to wash away unattached cells. Cell motility was observed under an inverted microscope. Images were recorded at 5-s intervals for 10 min by using a charge-coupled-device camera (Cool-SNAP EZ; Photometrics, Tucson, AZ) and were analyzed by using MetaMorph image analysis software (Molecular Devices, Downingtown, PA). Rainbow traces of cell movements were made by using ImageJ software (version 1.44p) (http://imagej.nih.gov/ij) and the Color Foot Print macro (29).

Western blot analyses. To prepare polyclonal antibodies against *C. ochracea* SprB, a peptide corresponding to residues 5271 to 5284 with an added N-terminal cysteine residue (CAGDYWYVLKTHEDG) was synthesized by means of 9-fluorenylmethoxy carbonyl (Fmoc) chemistry and was conjugated to keyhole limpet hemocyanin by using maleimidobenzoic acid *N*-hydroxysuccinimide ester purchased from Sigma-Aldrich. Rabbit immunization with the peptide conjugate, bleeding, and serum isolation were outsourced to Sigma-Aldrich. *C. ochracea* cells were grown to early stationary phase at 37°C in tryptic soy broth. The cells were then pelleted by centrifugation at 8,000 × *g* for 30 min, and the culture supernatants were collected. The supernatants (20 μg of protein) were separated by means of sodium dodecyl sulfate-polyacrylamide gel electrophoresis (5% gels; Cosmo Bio, Tokyo, Japan) under reducing conditions. After electrophoresis, the proteins were transferred onto polyvinylidene difluoride membranes (Bio-Rad), and SprB was detected by using the polyclonal antibodies (1:100 dilution).

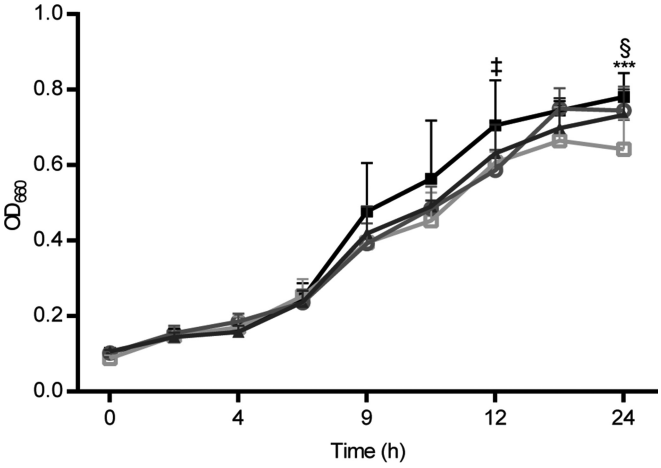

FIG 1 Growth curves for wild-type and ortholog-deficient mutant strains of *Capnocytophaga ochracea*. Wild-type *C. ochracea* ATCC 27872 (closed black squares), Δ*gldK* mutant (open light-gray squares), Δ*sprT* mutant (open gray circles), and Δ*sprB* mutant (closed dark-gray triangles) strains were grown at 37°C in tryptic soy broth supplemented with hemin and menadione under anaerobic conditions. Data are presented as means ± SDs ($n \geq 8$). ***, $P < 0.001$ (Δ*gldK* mutant versus wild-type strain); ‡, $P < 0.01$ (Δ*sprT* mutant versus wild-type strain); §, $P < 0.05$ (Δ*sprB* mutant versus wild-type strain).

Crystal violet biofilm formation assay. The biofilms formed by the *C. ochracea* strains were examined in 96-well polystyrene plates (Sumitomo Bakelite, Tokyo, Japan) as described previously, with minor modifications (20). Stationary-phase cultures of *C. ochracea* were adjusted to an OD_{660} of 0.1 with fresh tryptic soy broth. Cells were then added to 96-well plates (100 μl/well) and incubated for 48 h at 37°C under anaerobic conditions. Following incubation, the wells were washed three times with 200 μl of distilled water and stained with 50 μl of 0.1% crystal violet for 15 min at room temperature. After the crystal violet solution was removed and each well was washed twice with distilled water, the biomass-associated crystal violet was extracted with 200 μl of 99.5% ethanol. The extracted biomass-associated crystal violet (100 μl/well) was transferred to a new microtiter plate, and the OD_{595} was measured with a microplate reader (Spectra MAX M5e; Molecular Device, Sunnyvale, CA). Total biomass was calculated by using the following equation, which was described previously (36): total biomass = absorbance of crystal violet-stained biofilm at 595 nm/absorbance of total growth (including biofilm and planktonic cells) at 660 nm.

Confocal laser scanning microscopic analysis of biofilms. The biofilms produced by the *C. ochracea* strains were also examined by means of confocal laser scanning microscopy. One milliliter of cell suspension (OD_{660} of 0.1) was inoculated onto a plastic coverslip (Sumitomo Bakelite), in a 12-well polystyrene microtiter plate (BD Falcon, Franklin Lakes, NJ), at 37°C under anaerobic conditions. After 48 h, the medium was removed and the wells were washed three times with phosphate-buffered saline (PBS) (10 mM, pH 7.4; 2 ml/well) to remove unattached bacteria. The biofilms on the coverslips were fixed overnight at 4°C with 2% paraformaldehyde and 2.5% glutaraldehyde in PBS and were stained with the nucleic acid stains SYTO9 and propidium iodide by using the Live/Dead BacLight bacterial viability kit (Molecular Probes, Eugene, OR) according

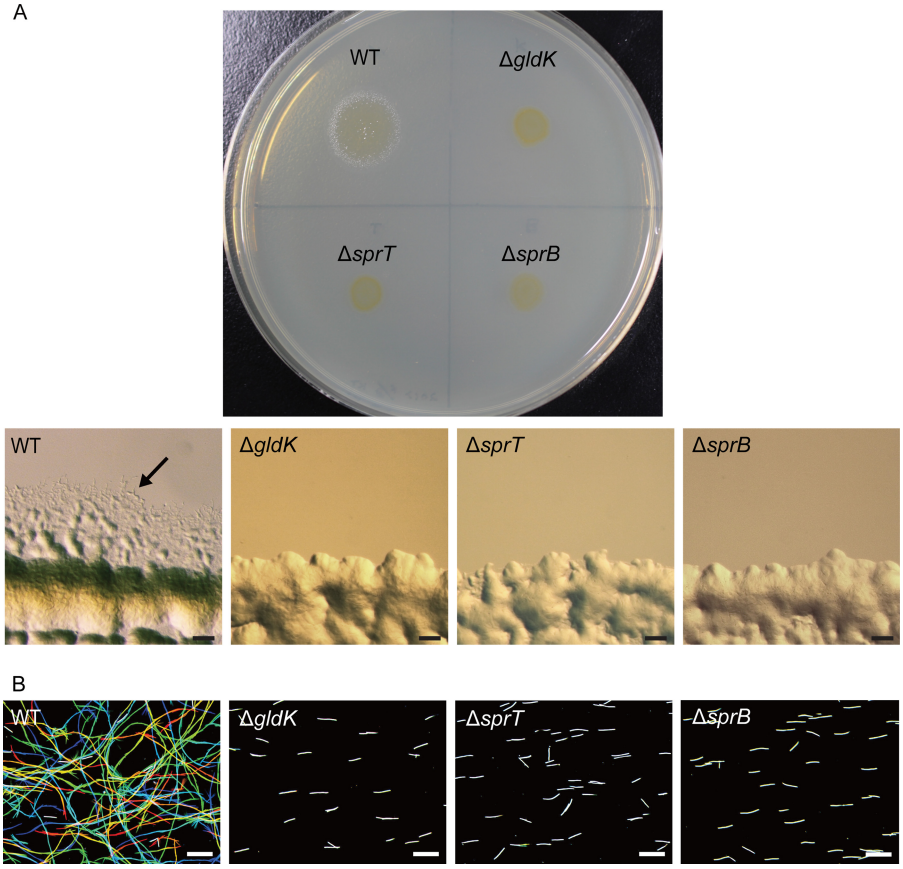

FIG 2 Effects of *gldK*, *sprT*, or *sprB* ortholog deficiency on gliding motility in *Capnocytophaga ochracea*. (A) Effects of *gldK*, *sprT*, or *sprB* ortholog deletion on colony spreading on a solid agar surface. Representative photographs of the colonies and photomicrographs of the edges of the colonies of each strain are shown. Black arrow, cells spreading away from the colony; scale bars, 100 μm. (B) Effects of *gldK*, *sprT*, or *sprB* ortholog deletion on gliding motility on a glass surface. Rainbow traces of cell movements were created with image analysis software. Nonmotile cells are shown in white. Scale bars, 10 μm. WT, wild-type *C. ochracea* ATCC 27872; Δ*gldK*, *gldK* ortholog-deficient *C. ochracea* mutant; Δ*sprT*, *sprT* ortholog-deficient *C. ochracea* mutant; Δ*sprB*, *sprB* ortholog-deficient *C. ochracea* mutant.

to the manufacturer's instructions. The biofilms were incubated in the dark at room temperature for 15 min, washed two times, and observed by means of confocal laser scanning microscopy, using a LSM5 DUO microscope (Carl Zeiss MicroImaging Inc., Göttingen, Germany) with a 63×/1.40 oil immersion objective. A series of z-stack images were scanned in increments of 0.1 μm, using excitation wavelengths of 489 and 532 nm. The images were analyzed using Zen 2009 (Carl Zeiss MicroImaging Inc.) and Imaris 7.0.0 (Bitplane AG, Zurich, Switzerland) software. Each z-stack image was further analyzed and quantified for biomass (total mass of living matter in a given unit area), average biofilm thickness, and maximum biofilm thickness by using the COMSTAT program (37).

Scanning electron microscopic analysis of biofilms. Samples were adjusted and incubated as described for the confocal laser scanning microscopic analysis. After 48 h, the medium was removed and the wells were washed once with PBS. Cells attached to the coverslips were fixed overnight at 4°C with 2% paraformaldehyde and 2.5% glutaraldehyde in PBS. The samples were washed twice with PBS and dehydrated in ethanol. The samples were then dried at the critical point of *t*-butyl alcohol, coated with gold/palladium by using a SC500A sputter coater (Bio-Rad), and observed under a scanning electron microscope (SU6600; Hitachi, Tokyo, Japan).

Biofilm stability. The stability of the biofilms produced by *C. ochracea* was examined by means of the crystal violet biofilm formation assay described above, with modification of the number of washes after removal of the medium, as described previously (38).

Biofilm detachment assay. Enzymatic treatment was carried out as described previously, with minor modifications (39, 40). Biofilms (produced by 100 μl of bacterial culture) were grown for 48 h in the wells of 96-well polystyrene microtiter plates, as described for the crystal violet biofilm formation assay. The biofilms were washed with 200 μl of distilled water and then treated overnight at 37°C with 200 μl of 0.5 mg/ml proteinase K (Roche Applied Sciences, Indianapolis, IN), DNase I (Roche Applied Sciences), or the carbohydrate-modifying agent sodium metaperiodate (Sigma-Aldrich) in PBS. Control wells received an equal volume of PBS. After treatment, the biofilms were washed twice with 200 μl of distilled water, stained with 50 μl of crystal violet, and then quantitated as described for the crystal violet biofilm formation assay.

Microscopic observation of bacterial attachment to a glass surface. Attachment of the *C. ochracea* strains to a glass surface was examined by using tunnel slides, as described previously (41). In brief, a stationary-phase culture of *C. ochracea* was adjusted to an OD_{660} of 0.5 with fresh tryptic soy broth, and 40 μl of the cell suspension was added to a tunnel slide. After 5 min, 200 μl of medium was added to wash away unattached cells. Cells attached to the slides were visualized under an inverted microscope (IX83; Olympus, Tokyo, Japan).

Autoaggregation assay. Autoaggregation of the *C. ochracea* strains was examined by using the assay described previously (20, 42). In brief, cells grown to stationary phase at 37°C under anaerobic conditions were washed twice with PBS and once with a coaggregation buffer consisting of 1 mM Tris-HCl (pH 8.0), 0.1 mM $CaCl_2$, 0.1 mM $MgCl_2$, and 150 mM

NaCl. Cells were resuspended to an OD_{660} of 0.5 in the same buffer. One milliliter of each cell suspension was placed in a cuvette, and the OD_{660} values at 0 and 120 min were determined with a spectrophotometer. The rate of autoaggregation was calculated by using the following equation: rate of autoaggregation = 100 − [(OD_{660} at 120 min/OD_{660} at 0 min) × 100].

Statistical analysis. Each experiment was performed independently at least twice. Results are expressed as mean values with standard deviations (SDs). One-way analysis of variance (ANOVA) with the Tukey-Kramer multiple-comparison test was used to determine differences between groups in the crystal violet biofilm formation assay. The Kruskal-Wallis test followed by Dunn's multiple-comparison test was used in the other experiments. *P* values of <0.05 were considered statistically significant. Statistical calculations were performed with the Prism software package (version 6.04; GraphPad Software, La Jolla, CA).

RESULTS

Growth of the Δ*gldK*, Δ*sprT*, and Δ*sprB* mutants. To determine the effects of *gldK*, *sprT*, or *sprB* ortholog deficiency on the growth of *C. ochracea*, the growth of the wild-type and mutant strains of *C. ochracea* was monitored under anaerobic conditions at 37°C. Significant differences in growth between the wild-type and mutant strains were observed during the late logarithmic and early stationary phases (Fig. 1).

Movement of the mutant strains on solid agar and glass surfaces. To investigate the effects of *gldK*, *sprT*, or *sprB* ortholog deficiency on gliding motility, colony spreading of the wild-type and mutant strains on a solid agar surface was examined under a phase-contrast microscope (Fig. 2A). The wild-type strain formed colonies that exhibited marked spreading across the solid agar surface, whereas the mutant strains formed colonies that exhibited little spreading. The movement of the wild-type and mutant strains on a glass surface was also examined. The wild-type strain exhibited movement over the glass surface, but the mutant strains did not (Fig. 2B). Together, these results indicate that SprB is crucial for the movement of *C. ochracea* across solid surfaces and that SprB is secreted via the T9SS.

Involvement of SprT in the secretion of SprB. In *F. johnsoniae*, T9SS proteins such as GldK, GldL, and SprT are necessary for secretion of the gliding motility adhesin SprB (30). Therefore, we examined the role of SprT in the secretion of SprB in *C. ochracea* by means of Western blotting (Fig. 3). SprB was detected in the culture supernatant of the wild-type strain but not in the supernatant of the Δ*sprT* mutant, indicating that the Δ*sprT* mutant did not secrete SprB. The size of the band detected was approximately equal to the estimated molecular mass of SprB (564,410.11 Da).

Biofilm formation by the mutant strains. Each mutant strain showed significantly attenuated biofilm formation, compared with that of the wild-type strain (Fig. 4A and B). The amounts of crystal violet-associated biomass for the Δ*gldK*, Δ*sprT*, and Δ*sprB* strains at 48 h were 49%, 34%, and 65% of that for the wild-type strain, respectively, indicating that the T9SS was involved in biofilm formation. To investigate further the effects of *gldK*, *sprT*, or *sprB* ortholog deficiency on biofilm formation, we examined the three-dimensional structures of the biofilms by means of confocal laser scanning microscopy and the COMSTAT program. The wild-type biofilm appeared denser than the mutant biofilms (Fig. 4C), and the biomass, average thickness, and maximum thickness of the Δ*gldK*, Δ*sprT*, and Δ*sprB* biofilms were significantly smaller than those of the wild-type biofilm (Fig. 4D). Furthermore, the amounts of crystal violet-associated biomass and the average and maximum thicknesses of the Δ*gldK* and Δ*sprT* biofilms were significantly smaller than those of the Δ*sprB* biofilm (Fig. 4A and D). Together, these results indicate not only that SprB secreted via the T9SS is involved in biofilm formation but also that, because biofilm formation was not completely attenuated, other proteins are involved in biofilm formation by *C. ochracea*.

FIG 3 Western blot analysis of the culture supernatants of wild-type *Capnocytophaga ochracea* ATCC 27872 and the Δ*sprT* mutant. The culture supernatants were subjected to sodium dodecyl sulfate-polyacrylamide gel electrophoresis and Western blot analysis with an antibody against SprB. Lane M, molecular size marker; lane WT, wild-type *C. ochracea* ATCC 27872; lane Δ*sprT*, *sprT* ortholog-deficient *C. ochracea* mutant. The size of the band observed for wild-type *C. ochracea* was approximately equal to the estimated molecular mass of SprB (564,410.11 Da).

Scanning electron microscopic analysis of the structure of biofilms. Bacterial biofilms are usually supported by a matrix of biopolymers known as extracellular polymeric substances (EPSs) (43). We next used a scanning electron microscope to analyze the structures of the biofilms formed by the *C. ochracea* strains. The wild-type strain formed a denser biofilm, with the cells packed together more closely, than did the mutant strains (Fig. 5).

Stability of the biofilms produced by the mutant strains. To investigate the stability of the biofilms produced by the mutants, the crystal violet biofilm formation assay was used but with different amounts of washing (Fig. 6). After a single wash, the decreases

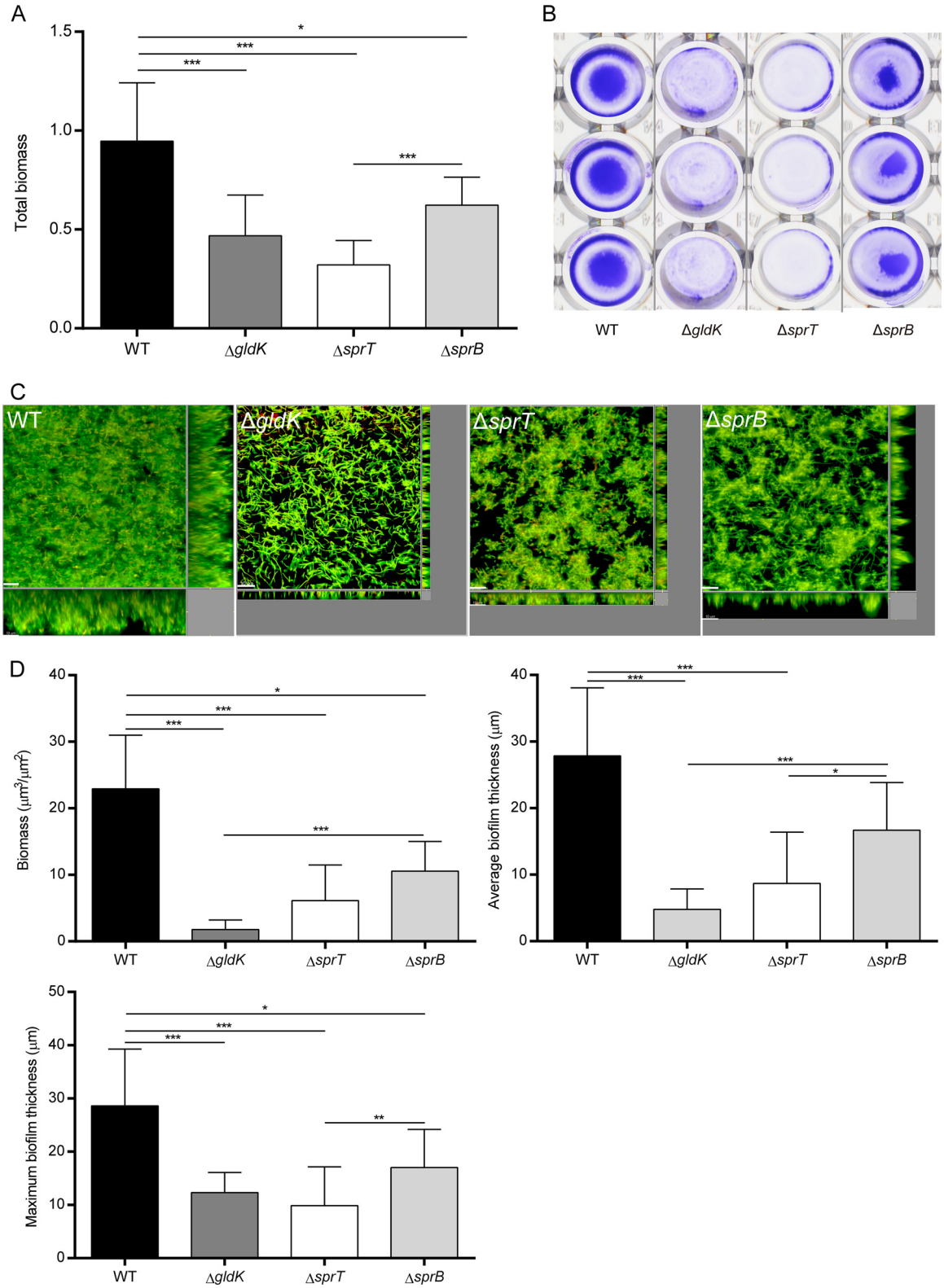

FIG 4 Effects of *gldK*, *sprT*, or *sprB* ortholog deficiency on biofilm formation by *Capnocytophaga ochracea*. (A) Total biomass of biofilms. Cells were incubated for 48 h at 37°C under anaerobic conditions, and the amount of biofilm produced was quantified by measuring the OD_{595} following crystal violet staining. Total biomass was calculated by using the following equation: total biomass = absorbance of crystal violet-stained biofilm at 595 nm/absorbance of total growth (including biofilm and planktonic cells) at 660 nm. Data are presented as means ± SDs ($n = 18$). *, $P < 0.05$; ***, $P < 0.001$. (B) Representative images of the results of the crystal violet biofilm formation assay. (C) Confocal laser scanning microscopic analysis of *C. ochracea* biofilms. *C. ochracea* strains were incubated for 48 h at 37°C under anaerobic conditions and were stained with the nucleic acid stains SYTO9 and propidium iodide. Images are presented as orthographic projections. (D) COMSTAT analyses of the three-dimensional structures of the biofilms produced by the wild-type and mutant strains of *C. ochracea*. Data are presented as means ± SDs ($n = 19$). *, $P < 0.05$; **, $P < 0.01$; ***, $P < 0.001$. WT, wild-type *C. ochracea* ATCC 27872; Δ*gldK*, *gldK* ortholog-deficient *C. ochracea* mutant; Δ*sprT*, *sprT* ortholog-deficient *C. ochracea* mutant; Δ*sprB*, *sprB* ortholog-deficient *C. ochracea* mutant. Scale bars, 10 μm.

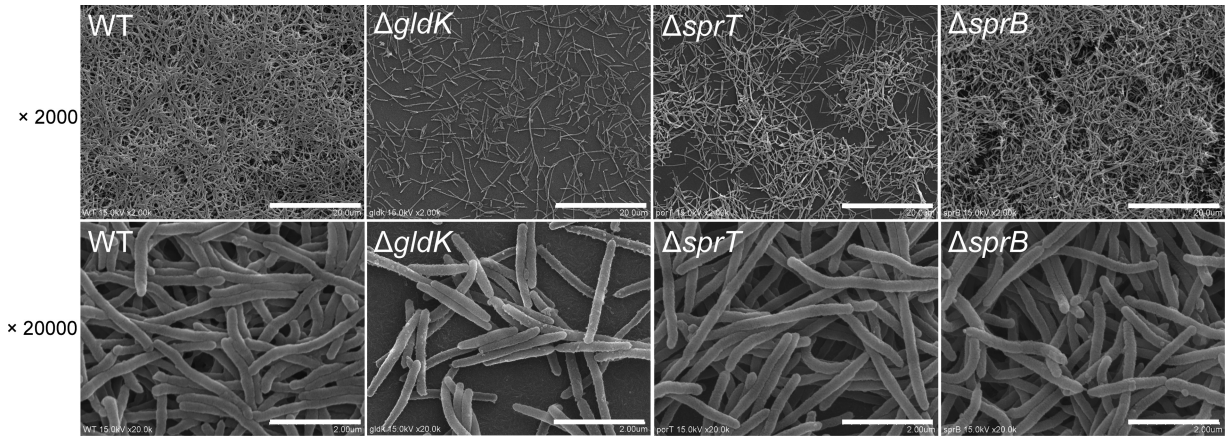

FIG 5 Scanning electron microscopic analysis of the structures of the *C. ochracea* biofilms. The biofilms were cultured at 37°C for 48 h before fixation. Scale bars, 20 μm for ×2,000 magnification and 2 μm for ×20,000 magnification. WT, wild-type *C. ochracea* ATCC 27872; Δ*gldK*, *gldK* ortholog-deficient *C. ochracea* mutant; Δ*sprT*, *sprT* ortholog-deficient *C. ochracea* mutant; Δ*sprB*, *sprB* ortholog-deficient *C. ochracea* mutant.

in the amounts of crystal violet-associated biomass were significantly greater for the Δ*gldK* and Δ*sprT* strains than for the wild-type strain. After three washes, the decreases in the amounts of crystal violet-associated biomass for all mutant strains were significantly greater than that for the wild-type strain. These results indicate that deletion of *gldK*, *sprT*, or *sprB* in *C. ochracea* reduces the stability of the *C. ochracea* biofilm.

Enzyme treatment of biofilms. EPSs can be proteins, nucleic acids, or polysaccharides (44, 45). Therefore, to characterize the structure of the biofilm further, we treated mature *C. ochracea* biofilms with proteinase K, DNase I, or $NaIO_4$. Treatment with proteinase K significantly reduced the amounts of biofilm produced by the wild-type, Δ*sprT*, and Δ*sprB* strains, indicating that biofilms produced by these strains were predominantly proteinaceous (Fig. 7). DNase I treatment slightly reduced the amounts of biofilm produced by each strain, although not statistically significantly.

Attachment to a glass surface and autoaggregation of the mutant strains. The adherence of bacteria to a solid surface is the first step in biofilm formation (44). Therefore, the effects of *gldK*, *sprT*, or *sprB* ortholog deficiency on the ability of *C. ochracea* to attach to a glass surface were examined by means of phase-con-

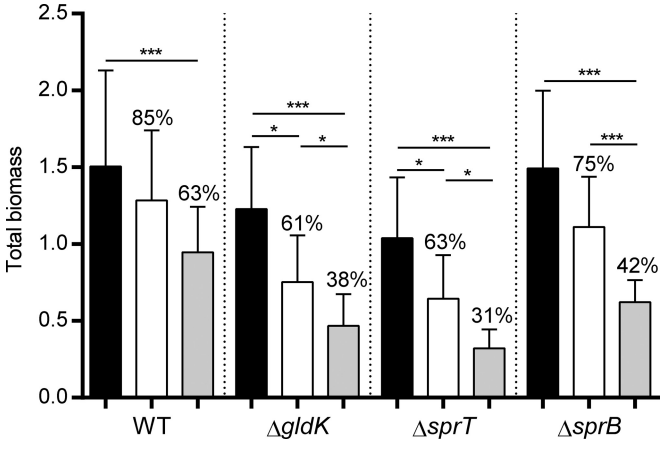

FIG 6 Effects of *sprT* or *sprB* ortholog deficiency on biofilm stability. *Capnocytophaga ochracea* biofilms were incubated for 48 h at 37°C under anaerobic conditions and then were washed a predetermined number of times. Black bar, 0 washes; white bar, 1 wash; light-gray bar, 3 washes. Percentages indicate the amounts of biomass remaining after each wash, calculated by using the following equation: (biomass remaining after each wash/biomass without washing) × 100. Data are presented as means ± SDs ($n = 18$). *, $P < 0.05$; ***, $P < 0.001$. WT, wild-type *C. ochracea* ATCC 27872; Δ*gldK*, *gldK* ortholog-deficient *C. ochracea* mutant; Δ*sprT*, *sprT* ortholog-deficient *C. ochracea* mutant; Δ*sprB*, *sprB* ortholog-deficient *C. ochracea* mutant.

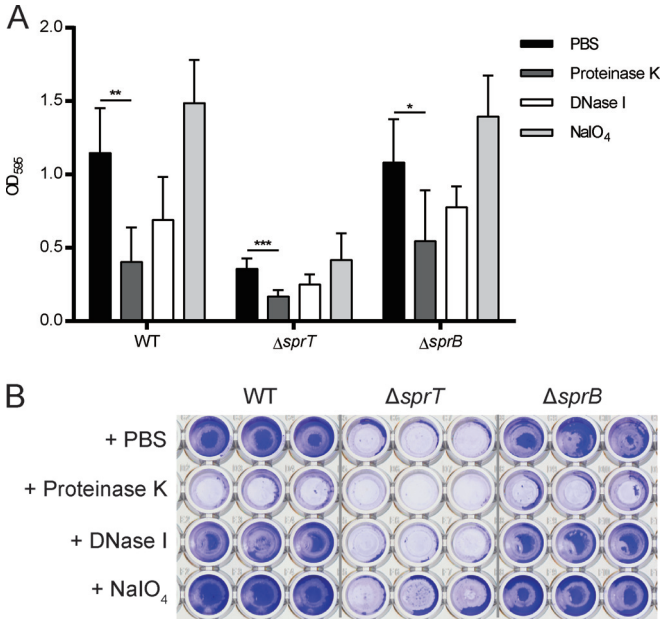

FIG 7 Effects of enzyme treatment on the biofilms produced by *Capnocytophaga ochracea*. (A) Total biomass of biofilms. Biofilms were grown for 48 h at 37°C under anaerobic conditions, treated with 0.5 mg/ml proteinase K, DNase I, or sodium metaperiodate ($NaIO_4$), and then incubated overnight at 37°C. After being washed, the biofilms were stained with 0.1% crystal violet. Data are presented as means ± SDs ($n = 9$). *, $P < 0.05$; **, $P < 0.01$; ***, $P < 0.001$. (B) Representative photographs of the results of crystal violet staining after enzymatic treatment of *C. ochracea* biofilms. WT, wild-type *C. ochracea* ATCC 27872; Δ*sprT*, *sprT* ortholog-deficient *C. ochracea* mutant; Δ*sprB*, *sprB* ortholog-deficient *C. ochracea* mutant.

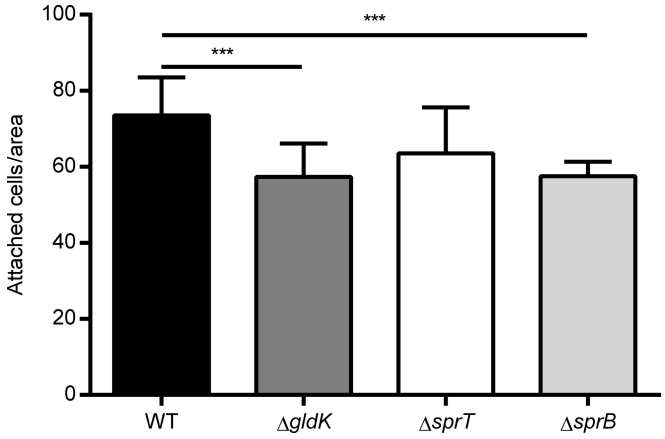

FIG 8 Effects of *gldK*, *sprT*, or *sprB* ortholog deficiency on the attachment of *Capnocytophaga ochracea* to a glass surface. The number of cells attached to the coverslip was counted. Data are presented as means ± SDs ($n = 15$). ***, $P < 0.001$. WT, wild-type *C. ochracea* ATCC 27872; Δ*gldK*, *gldK* ortholog-deficient *C. ochracea* mutant; Δ*sprT*, *sprT* ortholog-deficient *C. ochracea* mutant; Δ*sprB*, *sprB* ortholog-deficient *C. ochracea* mutant.

trast microscopy. Wild-type and Δ*sprT* strains exhibited comparable adherence to the glass surface; however, the Δ*gldK* and Δ*sprB* strains exhibited significantly less adherence than did the wild-type cells (Fig. 8).

Autoaggregation of the mutant strains was also examined, because it may play an important role in cellular adherence and biofilm formation (46). However, the autoaggregation rates of the wild-type, Δ*gldK*, Δ*sprT*, and Δ*sprB* strains were 6.7% ± 4.3%, 2.8% ± 2.5%, 5.7% ± 2.2%, and 7.0% ± 1.3%, respectively (data are presented as means ± SDs), indicating that autoaggregation was not affected by the deletion of *sprT* or *sprB*.

DISCUSSION

Bacterial surface molecules such as proteins are important for the attachment of bacterial cells to surfaces and for biofilm formation, because they interact directly with biotic or abiotic surfaces (47, 48). The T9SS is a major protein transport system for bacteria in the phylum *Bacteroidetes*, and it has been shown to be essential for the secretion of surface motility adhesins in *F. johnsoniae* (30). Here we demonstrated that GldK, SprT, and SprB were involved in the biofilm formation of *C. ochracea*.

Motility is an important factor for biofilm formation by Gram-negative bacteria. For *E. coli*, highly motile strains display biofilm structures that extend vertically, whereas strains with less motility display smoother microcolonies (49). A recent study with *Flavobacterium* spp. suggests that gliding motility is important for bacterial attachment to and colonization of plant surfaces (50). As *C. ochracea* demonstrates gliding motility, it is possible that this motility plays an important role in colonization on the tooth surface. In the present study, we showed that deletion of the *C. ochracea* orthologs of *gldK*, *sprT*, and *sprB* resulted in defective gliding motility on solid surfaces (Fig. 2). In *F. johnsoniae*, SprB is transported by the T9SS, is propelled along a left-handed helical loop on the cell surface, and is involved in gliding motility (25, 29). Similarly, the results of the present study indicate that SprB of *C. ochracea* is transported by the T9SS (Fig. 3) and is involved in gliding motility (Fig. 9). However, the detailed mechanism for the involvement of SprB in the gliding motility of *C. ochracea*, such as the movement of SprB on the cell surface, is unclear. The reductions in biofilm formation, relative to that of the wild-type strain, were greater for the Δ*gldK* and Δ*sprT* mutant strains than for the Δ*sprB* strain, even after correction for bacterial growth to avoid the effects of differences in growth rates (Fig. 4). This suggests that gliding motility is partly involved in biofilm formation by *C. ochracea* and that proteins exported by the T9SS other than SprB also play certain roles in biofilm formation.

Many bacteria that belong to the phylum *Bacteroidetes* secrete extracellular and surface proteins via the T9SS. The present data indicate that GldK and SprT, which are components of the T9SS (30), participate in biofilm formation. Several proteins with conserved C-terminal domain (CTD) regions, which are required for secretion by the T9SS, were detected in the genome sequence of *C. ochracea* (data not shown); these may be secreted by the T9SS. In the present study, Δ*gldK*, Δ*sprT*, and Δ*SprB* mutants showed a general trend for reductions in biofilm formation (Fig. 4) and adherence (Fig. 8), suggesting that the proteins secreted by the T9SS are involved in biofilm formation. It is important to note that the level of reduction of the Δ*gldK* mutant was somewhat low compared with that of the Δ*sprT* mutant. GldK is required for secretion by the *F. johnsoniae* T9SS, and SprT also has important roles in T9SS-mediated secretion. In *F. johnsoniae*, knockout of GldK completely inactivated T9SS function, but SprT knockout only partially inhibited it (30). This may be one reason for the

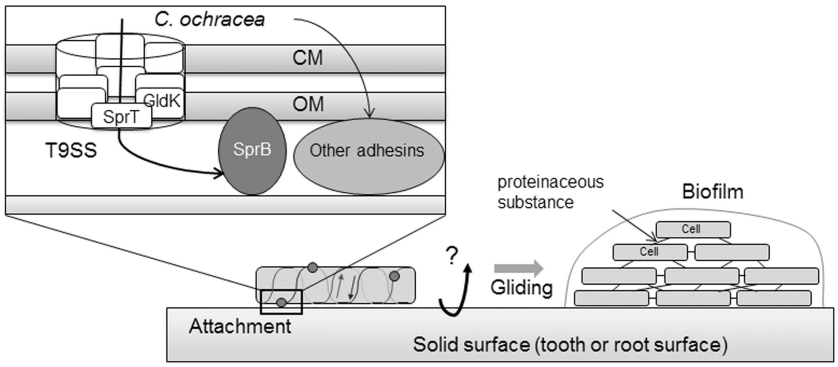

FIG 9 Model of the involvement of GldK, SprT, and SprB in attachment, gliding, and biofilm formation by *C. ochracea*. SprB is translocated to the cell surface and extracellular milieu via the T9SS. Subsequently, SprB attaches to and glides on solid surfaces (see the text for details). CM, cytoplasmic membrane; OM, outer membrane.

differences in the reductions of biofilm biomass and thickness in *C. ochracea*. These results collectively suggest that GldK and SprT participate in biofilm formation via T9SS-secreted proteins, including SprB (Fig. 9). Further study by proteomic analysis is necessary to clarify the locations of these proteins in the three-dimensional structure of the T9SS.

Bacterial adherence is another important factor for biofilm formation (51). Previous studies showed that Δ*gldK* and Δ*sprT* mutants of *F. johnsoniae* failed to attach to a glass surface (25, 30). In contrast, the ability of the Δ*gldK* mutant of *C. ochracea* to adhere to a glass surface decreased in the present study, but this decrease was much smaller than that for the Δ*gldK* mutant of *F. johnsoniae*. In addition, the ability of the Δ*sprT* mutant of *C. ochracea* to adhere to a glass surface was comparable to that of the wild-type strain (Fig. 8), suggesting that *C. ochracea* possesses other secretion systems that translocate adhesins to the cell surface and that *C. ochracea* GldK and SprT participate more in the maintenance of the three-dimensional architecture of the biofilm than in bacterial adhesion. Our results also indicate that autoaggregation does not play a major role in biofilm formation by *C. ochracea*.

Generally, biofilms cannot be removed easily by fluid shear stress (44). In the present study, however, the amounts of Δ*gldK* and Δ*sprT* biofilms remaining after washing were dramatically decreased, compared with the wild-type biofilm (Fig. 6). This result confirms that, in *C. ochracea*, GldK and SprT are involved in the maintenance of the biofilm architecture. In contrast, the amount of biofilm formed by the Δ*sprB* mutant was significantly decreased after three washes but not after one wash (Fig. 5 to 7), suggesting that, in *C. ochracea*, SprB also participates in the maintenance of the biofilm architecture. However, the degree of involvement of SprB in the maintenance of the biofilm architecture is likely less than that of GldK or SprT, which is reasonable, given that SprB is one of the proteins secreted via the T9SS. The present results also indicate that there are other substances secreted via the T9SS that are crucial for the maintenance of the biofilm architecture, because biofilm formation was not completely attenuated in the mutants.

EPSs provide mechanical stability for bacterial biofilms, keep bacterial cells in close proximity, mediate bacterial adhesion to surfaces, and form a cohesive, three-dimensional, polymer network that interconnects and transiently immobilizes cells within the biofilm (43). Our scanning electron microscopic analysis indicated that, compared with biofilms produced by the mutant strains, the wild-type biofilm was denser and bacterial cells were closer together (Fig. 5). Therefore, these results suggest that the differences in EPSs are responsible for the observed differences in biofilms. Moreover, treatment with proteinase K significantly reduced the total mass of the *C. ochracea* biofilm, whereas treatment with DNase I or $NaIO_4$ did not (Fig. 7), indicating that the main components of the biofilm were proteinaceous and the proteinaceous substances were responsible for the strength and amounts of the biofilm produced by *C. ochracea* (Fig. 9). We treated the biofilm with $NaIO_4$ to investigate the existence of polysaccharide in EPSs, because it was reported that *C. ochracea* produces exopolysaccharide containing large amounts of mannose, with smaller quantities of glucose, galactose, glucuronic acid, and glucosamine (52, 53). $NaIO_4$ oxidizes acidic polysaccharides and destroys their mannose residues (54). The results suggest that the mannose-rich exopolysaccharide was not the major component in the biofilm architecture. However, the results are not sufficient to rule out the involvement of other types of polysaccharides in the biofilm architecture. Further analysis with a staining procedure is necessary.

Altered biofilm formation by T9SS-component mutants has been reported for *Tannerella forsythia*, an important periodontal pathogen (36, 55, 56). The *T. forsythia* mutants lacked the surface layer (S-layer), which contains the cell surface glycoproteins TfsA and TfsB (36, 56). The S-layer is known to participate in *T. forsythia* adhesion to and invasion of host cells and in *T. forsythia*-mediated suppression of proinflammatory cytokine expression. A *T. forsythia* mutant deficient in the S-layer exhibited decreased hemagglutination and increased biofilm formation (36, 56). These findings contradict our observation that the amounts of biofilm formed by the *C. ochracea* mutant strains were smaller than the amount formed by the wild-type strain. This difference may be attributable to whether the bacteria possess an S-layer, but further analysis is required to understand the differences in biofilm formation between the *T. forsythia* and *C. ochracea* mutant strains. Analysis of the biofilms formed by T9SS-component mutants of other members of the phylum *Bacteroidetes* may also help us to understand in detail the role of the T9SS in biofilm formation.

In the present study, we demonstrated the involvement of the T9SS in *C. ochracea* biofilm formation. *C. ochracea* is found mainly in the oral cavity and is known to coaggregate with *F. nucleatum* (1, 20, 51). In dental plaque biofilms, *F. nucleatum* is a core bacterium for the growth of periodontopathic bacteria, including *Porphyromonas*, *Fusobacterium*, and *Prevotella* spp. It was recently reported that *Capnocytophaga* spp. increase their dominance within the bacterial community as dental plaque matures (57). Furthermore, a number of other bacteria, including major periodontal pathogens, have been found to harbor T9SS-related genes (28). Therefore, inhibitors of the T9SS represent a potential means of controlling the development of periodontopathic biofilms. Further clarification of the roles of the T9SS in periodontal pathogens is now needed.

ACKNOWLEDGMENTS

We thank Kazuko Okamoto-Shibayama for helpful discussions and Tomomi Kawana, Yoshiaki Kitazawa, and Katsumi Tadokoro for technical assistance.

FUNDING INFORMATION

Japan Society for the Promotion of Science (JSPS) provided funding to Kazuyuki Ishihara via a Grant-in-Aid for Scientific Research (C) (no. 24592778). JSPS provided funding to Atsushi Saito via a Grant-in-Aid for Scientific Research (C) (no. 25463228).

REFERENCES

1. **Mavrommatis K, Gronow S, Saunders E, Land M, Lapidus A, Copeland A, Glavina Del Rio T, Nolan M, Lucas S, Chen F, Tice H, Cheng JF, Bruce D, Goodwin L, Pitluck S, Pati A, Ivanova N, Chen A, Palaniappan K, Chain P, Hauser L, Chang YJ, Jeffries CD, Brettin T, Detter JC, Han C, Bristow J, Goker M, Rohde M, Eisen JA, Markowitz V, Kyrpides NC, Klenk HP, Hugenholtz P.** 2009. Complete genome sequence of *Capnocytophaga ochracea* type strain (VPI 2845). Stand Genomic Sci **1:**101–109. http://dx.doi.org/10.4056/sigs.15195.
2. **Leadbetter E, Holt S, Socransky S.** 1979. *Capnocytophaga*: new genus of Gram-negative gliding bacteria. I. General characteristics, taxonomic considerations and significance. Arch Microbiol **122:**9–16. http://dx.doi.org/10.1007/BF00408040.
3. **Poirier TP, Tonelli SJ, Holt SC.** 1979. Ultrastructure of gliding bacteria: scanning electron microscopy of *Capnocytophaga sputigena*, *Capnocy-*

tophaga gingivalis, and *Capnocytophaga ochracea*. Infect Immun **26:**1146–1158.
4. **Newman MG, Socransky SS.** 1977. Predominant cultivable microbiota in periodontosis. J Periodont Res **12:**120–128. http://dx.doi.org/10.1111/j.1600-0765.1977.tb00114.x.
5. **Slots J.** 1979. Subgingival microflora and periodontal disease. J Clin Periodontol **6:**351–382. http://dx.doi.org/10.1111/j.1600-051X.1979.tb01935.x.
6. **Williams BL, Ebersole JL, Spektor MD, Page RC.** 1985. Assessment of serum antibody patterns and analysis of subgingival microflora of members of a family with a high prevalence of early-onset periodontitis. Infect Immun **49:**742–750.
7. **Kobayashi N, Ishihara K, Sugihara N, Kusumoto M, Yakushiji M, Okuda K.** 2008. Colonization pattern of periodontal bacteria in Japanese children and their mothers. J Periodont Res **43:**156–161. http://dx.doi.org/10.1111/j.1600-0765.2007.01005.x.
8. **Duran-Pinedo AE, Chen T, Teles R, Starr JR, Wang X, Krishnan K, Frias-Lopez J.** 2014. Community-wide transcriptome of the oral microbiome in subjects with and without periodontitis. ISME J **8:**1659–1672. http://dx.doi.org/10.1038/ismej.2014.23.
9. **Kumar PS, Griffen AL, Barton JA, Paster BJ, Moeschberger ML, Leys EJ.** 2003. New bacterial species associated with chronic periodontitis. J Dent Res **82:**338–344. http://dx.doi.org/10.1177/154405910308200503.
10. **Paster BJ, Boches SK, Galvin JL, Ericson RE, Lau CN, Levanos VA, Sahasrabudhe A, Dewhirst FE.** 2001. Bacterial diversity in human subgingival plaque. J Bacteriol **183:**3770–3783. http://dx.doi.org/10.1128/JB.183.12.3770-3783.2001.
11. **Colombo AP, Haffajee AD, Dewhirst FE, Paster BJ, Smith CM, Cugini MA, Socransky SS.** 1998. Clinical and microbiological features of refractory periodontitis subjects. J Clin Periodontol **25:**169–180. http://dx.doi.org/10.1111/j.1600-051X.1998.tb02424.x.
12. **Moore WE, Moore LV.** 1994. The bacteria of periodontal diseases. Periodontol 2000 **5:**66–77. http://dx.doi.org/10.1111/j.1600-0757.1994.tb00019.x.
13. **Dzink JL, Socransky SS, Haffajee AD.** 1988. The predominant cultivable microbiota of active and inactive lesions of destructive periodontal diseases. J Clin Periodontol **15:**316–323. http://dx.doi.org/10.1111/j.1600-051X.1988.tb01590.x.
14. **Bolton RW, Kluever EA, Dyer JK.** 1985. In vitro immunosuppression mediated by an extracellular polysaccharide from *Capnocytophaga ochracea*: influence of macrophages. J Periodont Res **20:**251–259. http://dx.doi.org/10.1111/j.1600-0765.1985.tb00432.x.
15. **Ochiai K, Senpuku H, Kurita-Ochiai T.** 1998. Purification of immunosuppressive factor from *Capnocytophaga ochracea*. J Med Microbiol **47:**1087–1095. http://dx.doi.org/10.1099/00222615-47-12-1087.
16. **Desai SS, Harrison RA, Murphy MD.** 2007. *Capnocytophaga ochracea* causing severe sepsis and purpura fulminans in an immunocompetent patient. J Infect **54:**e107–e109. http://dx.doi.org/10.1016/j.jinf.2006.06.014.
17. **Piau C, Arvieux C, Bonnaure-Mallet M, Jolivet-Gougeon A.** 2013. *Capnocytophaga* spp. involvement in bone infections: a review. Int J Antimicrob Agents **41:**509–515. http://dx.doi.org/10.1016/j.ijantimicag.2013.03.001.
18. **Beck JD, Eke P, Heiss G, Madianos P, Couper D, Lin D, Moss K, Elter J, Offenbacher S.** 2005. Periodontal disease and coronary heart disease: a reappraisal of the exposure. Circulation **112:**19–24. http://dx.doi.org/10.1161/CIRCULATIONAHA.104.511998.
19. **Szymula A, Rosenthal J, Szczerba BM, Bagavant H, Fu SM, Deshmukh US.** 2014. T cell epitope mimicry between Sjogren's syndrome antigen A (SSA)/Ro60 and oral, gut, skin and vaginal bacteria. Clin Immunol **152:**1–9. http://dx.doi.org/10.1016/j.clim.2014.02.004.
20. **Okuda T, Okuda K, Kokubu E, Kawana T, Saito A, Ishihara K.** 2012. Synergistic effect on biofilm formation between *Fusobacterium nucleatum* and *Capnocytophaga ochracea*. Anaerobe **18:**157–161. http://dx.doi.org/10.1016/j.anaerobe.2012.01.001.
21. **Pratt LA, Kolter R.** 1998. Genetic analysis of *Escherichia coli* biofilm formation: roles of flagella, motility, chemotaxis and type I pili. Mol Microbiol **30:**285–293. http://dx.doi.org/10.1046/j.1365-2958.1998.01061.x.
22. **Costerton JW, Stewart PS, Greenberg EP.** 1999. Bacterial biofilms: a common cause of persistent infections. Science **284:**1318–1322. http://dx.doi.org/10.1126/science.284.5418.1318.
23. **Sato K, Yukitake H, Narita Y, Shoji M, Naito M, Nakayama K.** 2013. Identification of *Porphyromonas gingivalis* proteins secreted by the Por secretion system. FEMS Microbiol Lett **338:**68–76. http://dx.doi.org/10.1111/1574-6968.12028.
24. **Shoji M, Sato K, Yukitake H, Kondo Y, Narita Y, Kadowaki T, Naito M, Nakayama K.** 2011. Por secretion system-dependent secretion and glycosylation of *Porphyromonas gingivalis* hemin-binding protein 35. PLoS One **6:**e21372. http://dx.doi.org/10.1371/journal.pone.0021372.
25. **Sato K, Naito M, Yukitake H, Hirakawa H, Shoji M, McBride MJ, Rhodes RG, Nakayama K.** 2010. A protein secretion system linked to bacteroidete gliding motility and pathogenesis. Proc Natl Acad Sci U S A **107:**276–281. http://dx.doi.org/10.1073/pnas.0912010107.
26. **Sato K, Sakai E, Veith PD, Shoji M, Kikuchi Y, Yukitake H, Ohara N, Naito M, Okamoto K, Reynolds EC, Nakayama K.** 2005. Identification of a new membrane-associated protein that influences transport/maturation of gingipains and adhesins of *Porphyromonas gingivalis*. J Biol Chem **280:**8668–8677. http://dx.doi.org/10.1074/jbc.M413544200.
27. **Kharade SS, McBride MJ.** 2014. *Flavobacterium johnsoniae* chitinase ChiA is required for chitin utilization and is secreted by the type IX secretion system. J Bacteriol **196:**961–970. http://dx.doi.org/10.1128/JB.01170-13.
28. **McBride MJ, Zhu Y.** 2013. Gliding motility and Por secretion system genes are widespread among members of the phylum *Bacteroidetes*. J Bacteriol **195:**270–278. http://dx.doi.org/10.1128/JB.01962-12.
29. **Nakane D, Sato K, Wada H, McBride MJ, Nakayama K.** 2013. Helical flow of surface protein required for bacterial gliding motility. Proc Natl Acad Sci U S A **110:**11145–11150. http://dx.doi.org/10.1073/pnas.1219753110.
30. **Shrivastava A, Johnston JJ, van Baaren JM, McBride MJ.** 2013. *Flavobacterium johnsoniae* GldK, GldL, GldM, and SprA are required for secretion of the cell surface gliding motility adhesins SprB and RemA. J Bacteriol **195:**3201–3212. http://dx.doi.org/10.1128/JB.00333-13.
31. **Nelson SS, Bollampalli S, McBride MJ.** 2008. SprB is a cell surface component of the *Flavobacterium johnsoniae* gliding motility machinery. J Bacteriol **190:**2851–2857. http://dx.doi.org/10.1128/JB.01904-07.
32. **Fletcher HM, Schenkein HA, Morgan RM, Bailey KA, Berry CR, Macrina FL.** 1995. Virulence of a *Porphyromonas gingivalis* W83 mutant defective in the *prtH* gene. Infect Immun **63:**1521–1528.
33. **Shevchuk NA, Bryksin AV, Nusinovich YA, Cabello FC, Sutherland M, Ladisch S.** 2004. Construction of long DNA molecules using long PCR-based fusion of several fragments simultaneously. Nucleic Acids Res **32:**e19. http://dx.doi.org/10.1093/nar/gnh014.
34. **Ji X, Bai X, Li Z, Wang S, Guan Z, Lu X.** 2013. A novel locus essential for spreading of *Cytophaga hutchinsonii* colonies on agar. Appl Microbiol Biotechnol **97:**7317–7324. http://dx.doi.org/10.1007/s00253-013-4820-2.
35. **Shrivastava A, Rhodes RG, Pochiraju S, Nakane D, McBride MJ.** 2012. *Flavobacterium johnsoniae* RemA is a mobile cell surface lectin involved in gliding. J Bacteriol **194:**3678–3688. http://dx.doi.org/10.1128/JB.00588-12.
36. **Narita Y, Sato K, Yukitake H, Shoji M, Nakane D, Nagano K, Yoshimura F, Naito M, Nakayama K.** 2014. Lack of a surface layer in *Tannerella forsythia* mutants deficient in the type IX secretion system. Microbiology **160:**2295–2303. http://dx.doi.org/10.1099/mic.0.080192-0.
37. **Heydorn A, Nielsen AT, Hentzer M, Sternberg C, Givskov M, Ersboll BK, Molin S.** 2000. Quantification of biofilm structures by the novel computer program COMSTAT. Microbiology **146:**2395–2407. http://dx.doi.org/10.1099/00221287-146-10-2395.
38. **Nilsson M, Chiang WC, Fazli M, Gjermansen M, Givskov M, Tolker-Nielsen T.** 2011. Influence of putative exopolysaccharide genes on *Pseudomonas putida* KT2440 biofilm stability. Environ Microbiol **13:**1357–1369. http://dx.doi.org/10.1111/j.1462-2920.2011.02447.x.
39. **Hansen H, Bjelland AM, Ronessen M, Robertsen E, Willassen NP.** 2014. LitR is a repressor of *syp* genes and has a temperature-sensitive regulatory effect on biofilm formation and colony morphology in *Vibrio* (*Aliivibrio*) *salmonicida*. Appl Environ Microbiol **80:**5530–5541. http://dx.doi.org/10.1128/AEM.01239-14.
40. **Kaplan JB, Velliyagounder K, Ragunath C, Rohde H, Mack D, Knobloch JK, Ramasubbu N.** 2004. Genes involved in the synthesis and degradation of matrix polysaccharide in *Actinobacillus actinomycetemcomitans* and *Actinobacillus pleuropneumoniae* biofilms. J Bacteriol **186:**8213–8220. http://dx.doi.org/10.1128/JB.186.24.8213-8220.2004.
41. **Weiss DG.** 2005. Video-enhanced contrast microscopy, p 57–65. *In* Ceils JE, Hunter T, Carter N, Shotton D, Small JV, Simons K (ed), Cell biology: a laboratory handbook, 3rd ed, vol 3. Academic Press, San Diego, CA.
42. **Honma K, Mishima E, Inagaki S, Sharma A.** 2009. The OxyR homologue

in *Tannerella forsythia* regulates expression of oxidative stress responses and biofilm formation. Microbiology **155:**1912–1922. http://dx.doi.org/10.1099/mic.0.027920-0.
43. **Flemming HC, Wingender J.** 2010. The biofilm matrix. Nat Rev Microbiol **8:**623–633.
44. **Palmer J, Flint S, Brooks J.** 2007. Bacterial cell attachment, the beginning of a biofilm. J Ind Microbiol Biotechnol **34:**577–588. http://dx.doi.org/10.1007/s10295-007-0234-4.
45. **Monds RD, O'Toole GA.** 2009. The developmental model of microbial biofilms: ten years of a paradigm up for review. Trends Microbiol **17:**73–87. http://dx.doi.org/10.1016/j.tim.2008.11.001.
46. **Basson A, Flemming LA, Chenia HY.** 2008. Evaluation of adherence, hydrophobicity, aggregation, and biofilm development of *Flavobacterium johnsoniae*-like isolates. Microb Ecol **55:**1–14. http://dx.doi.org/10.1007/s00248-007-9245-y.
47. **Rosan B, Lamont RJ.** 2000. Dental plaque formation. Microbes Infect **2:**1599–1607. http://dx.doi.org/10.1016/S1286-4579(00)01316-2.
48. **Chagnot C, Zorgani MA, Astruc T, Desvaux M.** 2013. Proteinaceous determinants of surface colonization in bacteria: bacterial adhesion and biofilm formation from a protein secretion perspective. Front Microbiol **4:**303.
49. **Wood TK, Gonzalez Barrios AF, Herzberg M, Lee J.** 2006. Motility influences biofilm architecture in *Escherichia coli*. Appl Microbiol Biotechnol **72:**361–367. http://dx.doi.org/10.1007/s00253-005-0263-8.
50. **Kolton M, Frenkel O, Elad Y, Cytryn E.** 2014. Potential role of flavobacterial gliding-motility and type IX secretion system complex in root colonization and plant defense. Mol Plant Microbe Interact **27:**1005–1013. http://dx.doi.org/10.1094/MPMI-03-14-0067-R.
51. **Kolenbrander PE, Palmer RJ, Jr, Periasamy S, Jakubovics NS.** 2010. Oral multispecies biofilm development and the key role of cell-cell distance. Nat Rev Microbiol **8:**471–480. http://dx.doi.org/10.1038/nrmicro2381.
52. **Dyer JK, Bolton RW.** 1985. Purification and chemical characterization of an exopolysaccharide isolated from *Capnocytophaga ochracea*. Can J Microbiol **31:**1–5. http://dx.doi.org/10.1139/m85-001.
53. **Bolton RW, Dyer JK.** 1983. Suppression of murine lymphocyte mitogen responses by exopolysaccharide from *Capnocytophaga ochracea*. Infect Immun **39:**476–479.
54. **Nhan L-B, Jann B, Jann K.** 1971. Immunochemistry of K antigens of *Escherichia coli*: the K29 antigen of *E. coli* 09:K29(A):H−. Eur J Biochem **21:**226–234.
55. **Sharma A.** 2010. Virulence mechanisms of *Tannerella forsythia*. Periodontol 2000 **54:**106–116. http://dx.doi.org/10.1111/j.1600-0757.2009.00332.x.
56. **Tomek MB, Neumann L, Nimeth I, Koerdt A, Andesner P, Messner P, Mach L, Potempa JS, Schaffer C.** 2014. The S-layer proteins of *Tannerella forsythia* are secreted via a type IX secretion system that is decoupled from protein *O*-glycosylation. Mol Oral Microbiol **29:**307–320. http://dx.doi.org/10.1111/omi.12062.
57. **Takeshita T, Yasui M, Shibata Y, Furuta M, Saeki Y, Eshima N, Yamashita Y.** 2015. Dental plaque development on a hydroxyapatite disk in young adults observed by using a barcoded pyrosequencing approach. Sci Rep **5:**8136. http://dx.doi.org/10.1038/srep08136.